

Resistivity minimum emerges in Anderson impurity model modified with Sachdev-Ye-Kitaev interaction

Lan Zhang(张欄), Yin Zhong(钟寅)†, and Hong-Gang Luo(罗洪刚)‡

Citation: Chin. Phys. B, 2021, 30 (**4**): 047106. DOI: 10.1088/1674-1056/abefcb
Journal homepage: http://cpb.iphy.ac.cn; http://iopscience.iop.org/cpb

What follows is a list of articles you may be interested in

Intercalation of van der Waals layered materials: A route towards engineering of electron correlation

Jingjing Niu(牛晶晶), Wenjie Zhang(章文杰), Zhilin Li(李治林), Sixian Yang(杨嗣贤), Dayu Yan(闫大禹), Shulin Chen(陈树林), Zhepeng Zhang(张哲朋), Yanfeng Zhang(张艳锋), Xinguo Ren(任新国), Peng Gao(高鹏), Youguo Shi(石友国), Dapeng Yu(俞大鹏), Xiaosong Wu(吴孝松)
Chin. Phys. B, 2020, 29 (**9**): 097104. DOI: 10.1088/1674-1056/abab85

Point-contact spectroscopy on antiferromagnetic Kondo semiconductors CeT_2Al$_{10}$ (T=Ru and Os)

Jie Li(李洁), Li-Qiang Che(车利强), Tian Le(乐天), Jia-Hao Zhang(张佳浩), Pei-Jie Sun(孙培杰), Toshiro Takabatake, Xin Lu(路欣)
Chin. Phys. B, 2020, 29 (**7**): 077103. DOI: 10.1088/1674-1056/ab8dab

Lifshitz transition in triangular lattice Kondo-Heisenberg model

Lan Zhang(张欄), Yin Zhong(钟寅), Hong-Gang Luo(罗洪刚)
Chin. Phys. B, 2020, 29 (**7**): 077102. DOI: 10.1088/1674-1056/ab8da4

Phase diagram, correlations, and quantum critical point in the periodic Anderson model

Jian-Wei Yang(杨建伟), Qiao-Ni Chen(陈巧妮)
Chin. Phys. B, 2018, 27 (**3**): 037101. DOI: 10.1088/1674-1056/27/3/037101

Antiferromagnetism and Kondo screening on a honeycomb lattice

Lin Heng-Fu, Tao Hong-Shuai, Guo Wen-Xiang, Liu Wu-Ming
Chin. Phys. B, 2015, 24 (**5**): 057101. DOI: 10.1088/1674-1056/24/5/057101

Resistivity minimum emerges in Anderson impurity model modified with Sachdev–Ye–Kitaev interaction*

Lan Zhang(张欄)[1], Yin Zhong(钟寅)[1,†], and Hong-Gang Luo(罗洪刚)[1,2,‡]

[1] School of Physical Science and Technology & Key Laboratory for Magnetism and Magnetic Materials of the Ministry of Education, Lanzhou University, Lanzhou 730000, China
[2] Beijing Computational Science Research Center, Beijing 100084, China

(Received 9 October 2020; revised manuscript received 20 January 2021; accepted manuscript online 18 March 2021)

We investigate a modified Anderson model at the large-N limit, where the Coulomb interaction is replaced by the Sachdev–Ye–Kitaev random interaction. The resistivity of conduction electron ρ_c has a minimum value around temperature $T^\star$, which is similar to the Kondo system, but the impurity electron's density of state $A_d(\omega)$ demonstrates no sharp-peak like the Kondo resonance around the Fermi surface. This provides a counterintuitive example where resistivity minimum exists without Kondo resonance. The impurity electron's entropy S_d and specific heat capacity C_v show a crossover from Fermi liquid to a non-Fermi liquid behavior dependent on temperature. The system is a Fermi liquid at $T < T^\star$, and becomes a non-Fermi liquid at $T > T^\star$, and then becomes a Fermi gas at sufficiently high temperatures $T \gg T^\star$. The non-Fermi liquid at the intermediate-T regime does not occur in the standard Anderson model. We also make a renormalization group analysis, which confirms the crossover from Fermi liquid to the non-Fermi behavior. It is emphasized that the resistivity minimum emerges in our model when the system behaves as a non-Fermi liquid rather than Fermi liquid, which provides an alternative example showing resistivity minimum in condensed matter physics.

Keywords: Anderson model, Sachdev–Ye–Kitaev interaction, non-Fermi liquid

PACS: 71.27.+a, 71.10.–w **DOI:** 10.1088/1674-1056/abefcb

1. Introduction

The Anderson model is at the heart position to understand Kondo physics and heavy fermion compounds.[1–7] As the first microscopic model for magnetic moments formation in metals, it implies that local moments form once the Coulomb interaction between d-electrons becomes large.[8] A low-energy effective Hamiltonian of the Anderson model is the Kondo model, which is derived from the Anderson model via the Schrieffer–Wolff transformation,[9] and it demonstrates that resistivity ultimately rises as temperature is lowered. This leads to the conduction electron's resistivity emerges minimum versus temperature, which is one of the characteristics of the Kondo effect.[10] Correspondingly, there presents a sharp-peak of the impurity electron's spectral function at the Fermi surface, i.e., a Kondo resonance, when the Kondo screening appears to quench the local moments.[6] The evolution from localized magnetic moment state to the non-magnetic state, i.e., from Landau Fermi liquid to the localized Landau Fermi liquid, is a crossover among some rare-earth alloy and actinide compounds.[5,6]

The Landau Fermi liquid theory has been the workhorse of the physics of interacting electrons for over 60 years.[11] However, some heavy-fermion quantum critical compounds such as $CeCu_{6-x}Au_x$, $YbRh_2Si_2$ and β-$YbAlB_4$ display the non-Fermi liquid (NFL) behavior in which the transport properties and specific heat capacity cannot be derived from the Fermi liquid (FL) theory.[12–14] This attracts much attention to the NFL behavior, and many theories have been proposed to interpret this phenomenon.[15–21] The lack of controlled theoretical techniques hinders the understanding of the strong electron correlation in the NFL; nevertheless, the invention of the Sachdev–Ye–Kitaev (SYK) model provides a chance to understand the correlation physics in related systems accurately since its solvable nature.[22–25]

The SYK model is a quantum many-body model with random all-to-all interactions for fermions, which was studied in the 1990s and later as models for novel NFL or spin-glass states.[26–32] It provides a solvable example in zero dimension and has been extended to higher dimensions.[33–39] In recent years, many exotic physical phenomena have been found in SYK models, e.g., supersymmetry,[40] quantum chaos,[34,41–43] many-body localization,[44,45] strongly correlated metal,[46,47] and quantum phase transition.[24,25,48–51]

In a recent work[52] with an aim to provide a solvable model for a heavy-fermion system, the standard periodic Anderson model was modified with the SYK random interaction. This modified model was found to have a low temperature FL, and more interestingly, an NFL solution at elevated temperature and the rising of resistivity at high temperature can

*Project supported by the National Natural Science Foundation of China (Grant Nos. 11674139, 11704166, and 11834005) and the Fundamental Research Funds for the Central Universities, China, and PCSIRT (Grant No. IRT-16R35).

†Corresponding author. E-mail: zhongy@lzu.edu.cn
‡Corresponding author. E-mail: luohg@lzu.edu.cn

© 2021 Chinese Physical Society and IOP Publishing Ltd

be attributed to the single SYK quantum impurity.[52] In the present paper, we consider the distinction between the impurity and the lattice models and study the SYK quantum impurity problem, modeled by the Anderson model with SYK random interaction. We call it Sachdev–Ye–Kitaev Anderson model (SYKAM). Importantly, SYKAM provides an interesting and counterintuitive example where resistivity minimum exists in the absence of Kondo resonance. In a conventional picture, the resistivity minimum is due to the formation of Kondo resonance.



Fig. 1. Schematic phase diagram of the SYKAM. Our system has an FL behavior at $T < T^\star$ and behaves like the NFL at $T > T^\star$, while it is FG at $T \gg T^\star$.

Under the large-N limit, the qualitative analysis of the conduction electron resistivity ρ_c elucidates that the SYKAM behaves as an FL when temperature $T < T^\star$ and is an NFL at temperature $T > T^\star$, where $T^\star$ is a scaling temperature. The quantitative calculation gives a phase diagram as shown in Fig. 1, where ρ_c exists a minimum at temperature $T^\star$, demonstrating SYKAM behaves as an FL when $T < T^\star$ and the NFL at low temperature $T > T^\star$, and at high temperature $T \gg T^\star$, a free Fermi gas (FG) forms in SYKAM. It is emphasized that the NFL does not display in the standard Anderson model. From impurity electron's entropy S_d and specific heat capacity C_v, a crossover, not a phase transition, exists between FL and the NFL. This is confirmed by a renormalization group (RG) analysis, whose flow equation is similar to the Kondo problem.[1–5]

What is the relation between the standard Anderson and the SYK model? Compared with the standard Anderson model, the SYK random interaction does not provide localized interaction to the onsite different impurity spin states, leading to no local moment forming in our model. The hybridization between conduction and impurity electrons contributes to extending the localized impurity electron's density of state (DOS) to the Lorentz-like lineshape, and the impurity electron has the scattering with conduction electron sea, but its DOS shows that there is no sharp-peak at the Fermi surface like the Kondo resonance.[5,6,53,54] The resistivity minimum emerges in our model when the system behaves as an NFL rather than FL, while the system is localized FL when it presents the resistivity minimum in the standard Anderson model. Compared with the SYK model, our model includes the hybridization between the conduction electrons and the impurity electron. Such hybridization has an effect on the transport property; the resistivity is a constant line when $V = 0$ and has the resistivity minimum when hybridization is available, which the random interaction SYK system does not have. Both the SYK model, the standard Anderson model, and our model have similar thermodynamic properties (the entropy and the specific heat capacity). Our model and the standard Anderson model have the resistivity minimum, but the resistivity minimum emerges in our model approaching the non-Fermi liquid regime. Since the resistivity minimum and the Kondo resonance are two characteristics of the Kondo effect, in which the conduction electron screens the impurity electron's local moments.[5,6,53,54] The Kondo resonance is the most important feature to detect Kondo screening, and the resistivity minimum may be not enough to interpret the Kondo effect.

The paper is organized as follows. In Section 2, we introduce SYKAM and derive self-energy and the impurity electron Green's function. In Section 3, we present the conduction electron resistivity ρ_c. In Section 4, we compute thermodynamical behaviors of our model, i.e., impurity electron's entropy S_d and its specific heat capacity C_v. In Section 5, we apply RG theory to analyze the above results. Finally, Section 6 is devoted to a brief conclusion and perspective.

2. Model and method

The Hamiltonian of SYKAM can be written as

$$\hat{H} = \sum_{kj} \varepsilon_k \hat{c}^\dagger_{kj} \hat{c}_{kj} + \sum_{kj} V_k \left(\hat{c}^\dagger_{kj} \hat{d}_j + \hat{d}^\dagger_j \hat{c}_{kj} \right) + E_d \sum_j \hat{d}^\dagger_j \hat{d}_j + \frac{1}{(2N)^{3/2}} \sum_{ijml} U_{ijml} \hat{d}^\dagger_i \hat{d}^\dagger_j \hat{d}_m \hat{d}_l. \quad (1)$$

Here $\hat{c}^\dagger_{kj}$ ($\hat{c}_{kj}$) and $\hat{d}^\dagger_j$ ($\hat{d}_j$) denote the creation (annihilation) operator of conduction and impurity electrons with pseudospin $j = 1, 2, \ldots, N$, respectively. In Eq. (1), conduction electrons have energy dispersion ε_k and hybridize with impurity electron via strength V_k. For simplicity, we assume $V_k = V$ for all momentum. The impurity electron has degenerated energy level E_d. In contrast to the usual Anderson impurity model with the on-site Hubbard interaction, there exists the SYK-like random all-to-all interaction U_{ijml} between different pseudospin states of impurity electron, wherein U_{ijml} satisfies a standard Gaussian random distribution $P(x) = \frac{1}{\sqrt{2\pi}U} \mathrm{e}^{-\frac{x^2}{2U^2}}$ with $\overline{U}_{ijml} = \int_{-\infty}^{\infty} \mathrm{d}U_{ijkl} P(U_{ijkl}) U_{ijkl} = 0$ and $\overline{U^2}_{ijml} = \int_{-\infty}^{\infty} \mathrm{d}U_{ijkl} P(U_{ijkl}) U^2_{ijkl} = U^2$, as shown in Fig. 2.

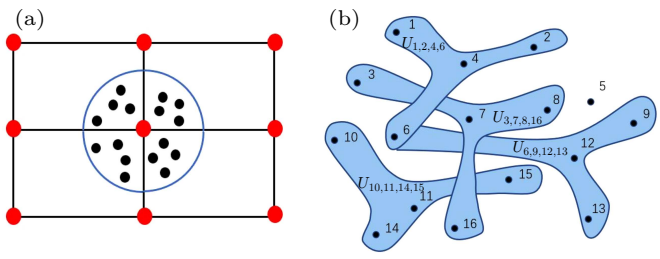


Fig. 2. (a) Schematic crystal lattice of SYKAM, where the red dots are the conduction electrons, and the black dots are the impurity electron pseudospin states. (b) The SYK random interaction U_{ijml} between different impurity electron pseudospin states $1, 2, \ldots, 16, \ldots, N$.

To solve the mentioned model Eq. (1), we consider the large-N limit as done in the SYK model, which means that the number of the component of pseudospin $j = 1, 2, \ldots, N$ is artificially enlarged to infinity. As a result, the partition function of our system can be approximated by its saddle point value (see the appendix). Equivalently, the large-N limit means that after the disorder average over U_{ijkl}, the self-energy of impurity electron $\Sigma(\mathrm{i}\omega_n)$ is dominated by the watermelon diagram as shown in Fig. 3,

$$\Sigma(\tau) = U^2 \left[G_{\mathrm{d}}(-\tau)\right]^2 G_{\mathrm{d}}(\tau). \tag{2}$$

Therefore, via the Dyson equation, the resulting Green's function for the impurity electron reads

$$G_{\mathrm{d}}(\mathrm{i}\omega_n) = \frac{1}{\mathrm{i}\omega_n - E_{\mathrm{d}} - \sum_k \frac{V^2}{\mathrm{i}\omega_n - \varepsilon_k} - \Sigma(\mathrm{i}\omega_n)}, \tag{3}$$

where $\omega_n = (2n+1)\pi T$ denotes the fermionic Matsubara frequency with $n = 0, \pm 1, \pm 2, \ldots, \pm\infty$.

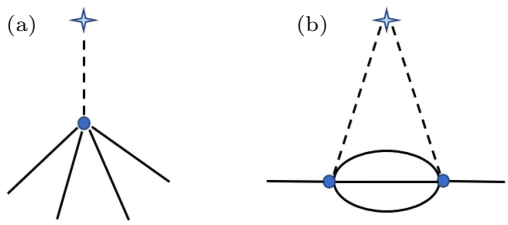


Fig. 3. The leading impurity electron self-energy Feynman diagrams for SYKAM under the large-N limit. (a) is the bare interaction vertex before average over random interaction U_{ijml}. (b) illustrates the self-energy after average.

For conduction electron, its Green's function $G_{\mathrm{c}}(k, \mathrm{i}\omega_n)$ is derived from the equation of motion[5] and reads

$$G_{\mathrm{c}}(k, \mathrm{i}\omega_n) = \frac{1}{\mathrm{i}\omega_n - \varepsilon_k} + \frac{V^2}{(\mathrm{i}\omega_n - \varepsilon_k)^2} G_{\mathrm{d}}(\mathrm{i}\omega_n). \tag{4}$$

Consequently, $G_{\mathrm{d}}(\mathrm{i}\omega_n)$ and $G_{\mathrm{c}}(k, \mathrm{i}\omega_n)$ can be found by solving Eqs. (2)–(4) self-consistently.

For simplicity, the DOS of conduction electrons is assumed to be $N(\varepsilon) = \frac{1}{2D}\theta(D - |\varepsilon|)$, with $\theta(x)$ being a step function, and $2D$ is the band-width of conduction electrons. Under the above assumption, the hybridization contribution to the impurity electron is

$$\sum_k \frac{V^2}{\mathrm{i}\omega_n - \varepsilon_k} = -V^2 N(0) \ln\left[\frac{D - \mathrm{i}\omega_n}{-D - \mathrm{i}\omega_n}\right]. \tag{5}$$

When $D \gg |\omega_n|$, we get

$$G_{\mathrm{d}}(\mathrm{i}\omega_n) = \frac{1}{\mathrm{i}\omega_n - E_{\mathrm{d}} + \mathrm{i}\Delta \mathrm{sgn}(\mathrm{i}\omega_n) - \Sigma(\mathrm{i}\omega_n)}, \tag{6}$$

where $\Delta = \pi V^2 N(0)$, and $N(0) = \frac{1}{2D}$ is the DOS of the conduction electron at Fermi energy.[55]

According to the Feynman diagrams, we can get the impurity electron self-energy

$$\Sigma(\mathrm{i}\omega_n) = U^2 \int \mathrm{d}\omega_1 \int \mathrm{d}\omega_2 \int \mathrm{d}\omega_3 \Big[A_{\mathrm{d}}(\omega_1) A_{\mathrm{d}}(\omega_2) A_{\mathrm{d}}(\omega_3) \times \frac{f(\omega_1) f(-\omega_2) f(-\omega_3) + f(-\omega_1) f(\omega_2) f(\omega_3)}{\mathrm{i}\omega_n + \omega_1 - \omega_2 - \omega_3}\Big], \tag{7}$$

where $f(x)$ is the Fermi–Dirac distribution function.

Therefore, we can obtain $G_{\mathrm{d}}(\mathrm{i}\omega_n)$ and $G_{\mathrm{c}}(k, \mathrm{i}\omega_n)$ by solving Eqs. (4), (6), and (7) self-consistently. Before presenting the numerical results, one can inspect two limiting cases (weak and strong coupling) and extract useful analytic formulas.

2.1. Weak coupling limit

In the weak coupling limit, the self-energy correction $\Sigma(\mathrm{i}\omega_n)$ is assumed to be small compared with the free part $\mathrm{i}\omega_n - E_{\mathrm{d}} + \mathrm{i}\Delta$ in $G_{\mathrm{d}}(\mathrm{i}\omega_n)$. At zero temperature, one can use non-interacting impurity electron Green's function

$$G^0_{\mathrm{d}}(\omega) = \frac{1}{\omega - E_{\mathrm{d}} + \mathrm{i}\Delta}, \tag{8}$$

and we use the analytic continuation $\mathrm{i}\omega_n \to \omega + \mathrm{i}\delta$ to get the zero temperature impurity electron self-energy

$$\Sigma(\omega) = U^2 \int \mathrm{d}\omega_1 \int \mathrm{d}\omega_2 \int \mathrm{d}\omega_3 \Big[A^0_{\mathrm{d}}(\omega_1) A^0_{\mathrm{d}}(\omega_2) A^0_{\mathrm{d}}(\omega_3) \times \frac{\theta(-\omega_1)\theta(\omega_2)\theta(\omega_3) + \theta(\omega_1)\theta(-\omega_2)\theta(-\omega_3)}{\omega + \mathrm{i}\delta + \omega_1 - \omega_2 - \omega_3}\Big], \tag{9}$$

with $A^0_{\mathrm{d}}(\omega) = \frac{1}{\pi}\frac{\Delta}{(\omega - E_{\mathrm{d}})^2 + \Delta^2}$, where δ denotes the infinitesimal positive parameter. To proceed, we set $E_{\mathrm{d}} = 0$ and consider the low-energy limit with $|\omega| \ll \Delta$, $A^0_{\mathrm{d}}(\omega) \approx 1/(\pi\Delta)$. Thus, the imaginary part of self-energy is approximated to be

$$\mathrm{Im}\Sigma(\omega) = -\frac{U^2\pi}{2(\pi\Delta)^3}\omega^2 + O(\omega^4) \propto \omega^2,$$

which indicates a local FL behavior.[56] Via the Kramers–Kronig relation, its real part is $\mathrm{Re}\Sigma(\omega) \propto \omega$.[6]

As a matter of fact, we can go beyond perturbation theory analysis by showing that FL-like Green's function $G_{\mathrm{d}}(\omega) = \frac{Z}{\omega + \mathrm{i}B\Delta}$ is the self-consistent solution if one inserts it into Eq. (9). As a result, one finds the quasiparticle weight $Z = 1/[1 + (\frac{U}{\pi\Delta})^2]$ and $B = Z$.

We conclude that the system behaves like a local FL in the weak coupling limit, which is similar to the ground state of the standard Anderson impurity model.[5]

2.2. Strong coupling limit

In the strong coupling limit, the self-energy correction $\Sigma(\mathrm{i}\omega_n)$ seems to be large. If $\Sigma(\mathrm{i}\omega_n) \gg \Delta$, one can approximate impurity electron Green's function as

$$G_{\mathrm{d}}(\mathrm{i}\omega_n) = -\frac{1}{\Sigma(\mathrm{i}\omega_n)},$$

which is identical to the cases in the SYK models. Thus, analytic continuation, the self-energy is found to be

$$\Sigma_{\rm SYK}(\omega)=-\frac{1}{\frac{\pi^{-1/4}}{\sqrt{2U}}\frac{\sqrt{\pi}}{\sqrt{|\omega|}}\theta(-\omega)-\mathrm{i}\frac{\pi^{-1/4}}{\sqrt{2U}}\frac{\sqrt{\pi}}{\sqrt{|\omega|}}\theta(\omega)},$$

the quasiparticle weight is defined as

$$Z=\frac{1}{1-\partial_\omega \mathrm{Re}\Sigma}\bigg|_{\omega\to 0}\propto\sqrt{\frac{|\omega|}{U}}\bigg|_{\omega\to 0}\to 0,$$

which corresponds to the NFL behavior.[38]

However, when comparing the SYK self-energy $\Sigma_{\rm SYK}(\omega)$ with the remaining hybridization term $\mathrm{i}\Delta$ in our model, we find the SYK physics dominates at high-energy regime $\omega>E^*$ while the FL-like behavior works if $\omega<E^*$. Here, $E^*\sim\Delta^2/U$ is obtained via $\Sigma_{\rm SYK}\sim\sqrt{U|\omega|}\sim\Delta$.

Therefore, at strong coupling, the self-energy should be approximated a mixture of FL and SYK form as

$$\Sigma_{\rm SYK}(\omega)\sim\theta(E^*-|\omega|)\Sigma_{\rm FL}(\omega)+\theta(|\omega|-E^*)\Sigma_{\rm SYK}(\omega), \quad (10)$$

where $\Sigma_{\rm FL}(\omega)$ has an FL-like form.

Combining the results from weak and strong coupling analysis, one finds that our system is always an (local) FL at low-temperature or low energy below a characteristic energy scale E^*. When elevating temperature or jumping into high energy regime above E^*, the NFL behavior is driven by the SYK interaction.

3. Transport properties

Before performing calculations of transport quantities, we inspect the behavior of the single-particle Green's functions.

$$E^\star=k_{\rm B}T^\star\sim\frac{\Delta^2}{U}, \quad (11)$$

and here we set Boltzmann's constant $k_{\rm B}=1$, we have

$$T^\star\sim\frac{\Delta^2}{U}. \quad (12)$$

At $|\omega|\gg E^\star$, the impurity electron Green's function is dominated by the self-energy term and has an NFL feature. When $|\omega|\ll E^\star$, it shows FL-like behavior, the detailed formulas of Green's function of the impurity electron and the conduction electron are given in the appendix.

Since the static resistivity is inversely proportional to the static limit of optical conductivity, we can compute the latter quantitatively via the Kubo formula[6]

$$\sigma_{xx}(\omega)=\frac{1}{\omega}\Pi''(\omega+\mathrm{i}\delta), \quad (13)$$

and

$$\Pi_{xx}(\omega)=-\mathrm{i}\int_0^\infty \mathrm{e}^{\mathrm{i}\omega t}\langle[\hat{J}_x(t),\hat{J}_x(0)]\rangle, \quad (14)$$

denotes the current–current response function. Here, the x-component of current operator $\hat{J}_x$ is given by[57]

$$\hat{J}_x=\frac{e}{\hbar}\sum_{kj}\frac{\partial\varepsilon_k}{\partial k_x}\hat{c}^\dagger_{kj}\hat{c}_{kj}, \quad (15)$$

where the conduction electron dispersion is $\varepsilon_k=2t\Sigma_{j=x,y,z}\cos(k_j a)$ with t the nearest-neighbor hopping, and a is the crystal constant. Inserting $G_{\rm c}(k,\omega)$ into $\sigma_{xx}(\omega)$, the static conductivity is

$$\begin{aligned}&\sigma_{xx}(\omega=0)\\&=\frac{e^2\pi}{\hbar^2}\sum_{kj}\int \mathrm{d}\varepsilon_1\left[-\frac{\mathrm{d}f}{\mathrm{d}\varepsilon_1}\right]\left(\frac{\partial\varepsilon_k}{\partial k_x}\right)^2[A_{\rm c}(k,\varepsilon_1)]^2,\end{aligned} \quad (16)$$

where the spectral function of conduction electrons is given in the appendix.

At zero temperature, the term $[-\mathrm{d}f/\mathrm{d}\varepsilon_1]$ becomes the delta function $\delta(\varepsilon_1)$, and the impurity electron DOS is

$$A_{\rm d}(\varepsilon_1)=-\frac{1}{\pi}\mathrm{Im}G_{\rm d}(\varepsilon_1+\mathrm{i}\delta)\propto\begin{cases}\frac{1}{\Delta}, & |\varepsilon_1|\ll E^\star,\\ \frac{1}{\sqrt{U|\varepsilon_1|}}, & |\varepsilon_1|\gg E^\star.\end{cases} \quad (17)$$

Thus, the resistivity is constant at zero temperature.

At finite temperature, we use Sommerfeld expansion to Eq. (16).[59] At low temperature, $f(\varepsilon_1)\propto 1/T^2$. At high temperature, we give the basic linear fitting as shown in Fig. 4. Thus, we have

$$\rho_{\rm c}(T)\propto\begin{cases}\frac{D^4\Delta^2}{V^4}-T^2, & T\ll T^\star,\\ T, & T>T^\star.\end{cases} \quad (18)$$

It means that our system behaves as FL at low temperature and has the NFL behavior at high temperature.

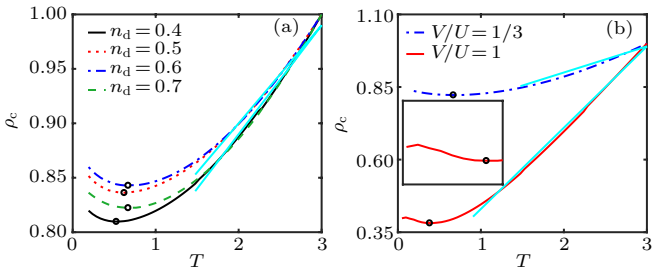


Fig. 4. The conduction electron resistivity $\rho_{\rm c}$ as a function of temperature T. For the different impurity electron concentrations $n_{\rm d}$ as shown in (a), the black dots are $T^\star=0.5246, 0.6198, 0.6674, 0.6674$ for $n_{\rm d}=0.4$, 0.5, 0.6, 0.7, and the parameters are $V=1, U=3, D=12, E_{\rm d}=-U/2$. In (b), $\rho_{\rm c}$ versus V/U at $n_{\rm d}=0.7$, the blue dashed line is the same as $n_{\rm d}=0.7$ in (a), and the red solid line is $V/U=1/3$ with $T^\star=0.3818$, the inset shows the low temperature case of $\rho_{\rm c}$, where parameters are $V=1, U=1, D=4, E_{\rm d}=-U/2$. The cyan lines are the basic linear fitting, which shows that $\rho_{\rm c}(T)\propto T$ at $T>T^\star$.

Due to the impurity, electron occupation $n_{\rm d}$ is

$$n_{\rm d}=\int \mathrm{d}\omega A_{\rm d}(\omega)f(\omega), \quad (19)$$

where $A_{\rm d}(\omega)$ is the spectral function of the impurity electron, $f(x)=1/[\mathrm{e}^{(x-\mu)/T}+1]$ is the Fermi–Dirac distribution function, μ is the system's chemical potential for both conduction

and the impurity electrons. Because the system has just one impurity electron with N pseudospins, we take the chemical potential as μ_c in our work. When we fixed the impurity electron occupation n_d, $A_d(\omega)$ and $f(\omega)$ change versus temperature T, and the conduction electron spectral function $A_c(k,\omega)$ also change according to Eq. (A4). From Eq. (16), we plot the conduction electron resistivity ρ_c versus T at the impurity electron occupation $n_d = 0.4, 0.5, 0.6, 0.7$, as shown in Fig. 4. For the case of the fixed conduction electron occupation, the detailed discussion is given in the appendix.

In Fig. 4, the conduction electron resistivity ρ_c has a minimum at $T^\star$, which is similar to the Kondo effect.[5,6,60] When temperature $T > T^\star$, the line of $n_d = 0.4$ coincides with $n_d = 0.7$, which is similar to $n_d = 0.5$ and $n_d = 0.6$. At low temperature $T < T^\star$, ρ_c is proportional to the square of temperature, which behaves as FL. However, four lines have linear resistivity at high temperature $T > T^\star$, where the system behaves as the NFL. In Fig. 4(b), it demonstrates that the line of $V/U = 1/3$ with $D = 12$ has a higher $T^\star$ than $V/U = 1$ with $D = 4$, where the wide bandwidth $2D$ and the large random interaction U also induces a high $T^\star$, which coincides with Eq. (12). The red solid line of Fig. 4(b) has the constant resistivity at low temperature as shown in the inset, which also demonstrates that our system has FL behavior at $T < T^\star$, and behaves like the NFL at $T > T^\star$ because of linear resistivity, when $T \gg T^\star$ the system has the FG behavior as shown in Fig. 1.

We also have shown the conduction electron resistivity ρ_c versus temperature T for $E_d = 0, U/2$ at different impurity concentrations $n_d = 0.4, 0.5, 0.6, 0.7$ in Fig. 5. Compared with Fig. 4, both resistivity lines have the minimum and the larger E_d induces the smaller $T^\star$. It demonstrates that SYKAM is not symmetric around $n_d = 0.5$. Our model is different from the single-impurity Anderson model; the symmetric Anderson model $E_d = -U/2$ has the particle-hole symmetry around $n_d = 0.5$.[5] However, our model has the four-body SYK random all-to-all interaction, in contrast to the onsite two-body Coulomb interaction, which is not satisfied with the particle-hole symmetry except for the case $U_{ijml} = 0$.

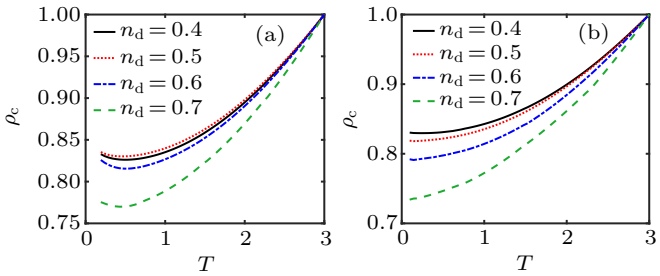


Fig. 5. The conduction electron resistivity ρ_c as a function of temperature T for the different impurity electron concentrations $n_d = 0.4$, 0.5, 0.6, 0.7, respectively. (a) is the case $E_d = 0$. (b) is the case $E_d = 1.5$. The parameters are $V = 1$, $U = 3$, $D = 12$.

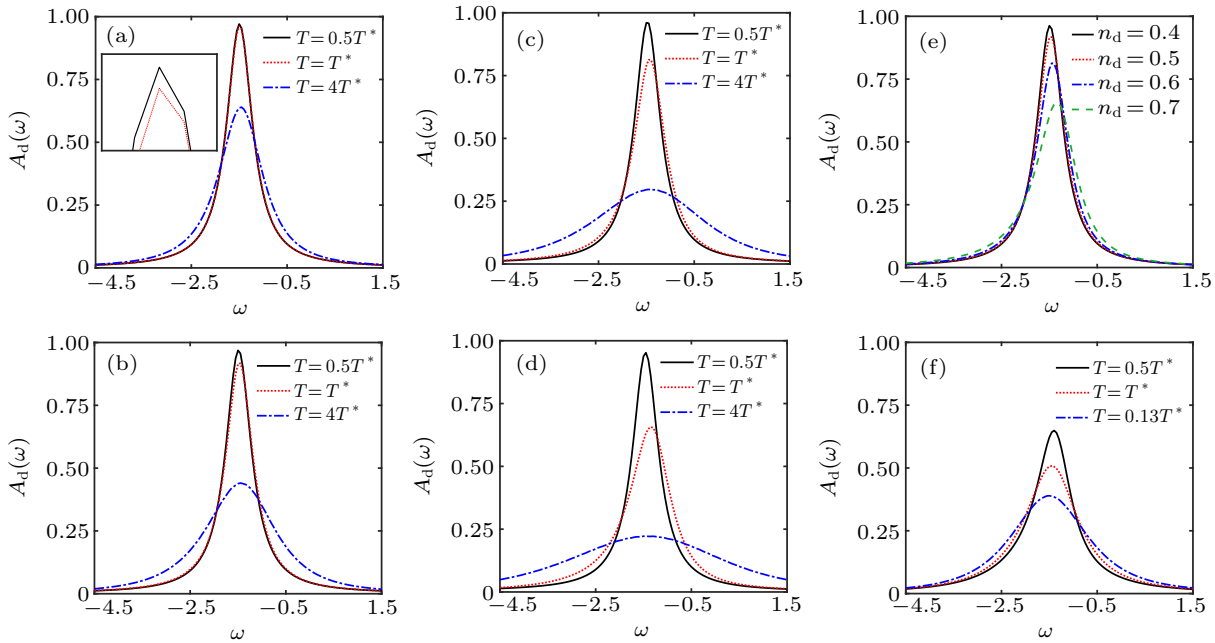


Fig. 6. The impurity electron DOS $A_d(\omega)$ as a function of the frequency ω. (a)–(d) are for different temperature T with the limited impurity electron concentrations $n_d = 0.4, 0.5, 0.6, 0.7$; the inset of (a) shows that two lines are not merged together. (e) describes $A_d(\omega)$ versus n_d at $T^\star = 0.5246, 0.6198, 0.6674, 0.6674$, respectively. The parameters of (a)–(e) are $V = 1$, $U = 3$, $D = 12$, $E_d = -U/2$. In (f), all lines are plotted with $V = 1$, $U = 1$, $D = 4$, $E_d = -U/2$ at $n_d = 0.7$, and $T^\star = 0.3818$, where the black solid line is the DOS of FL at the constant resistivity.

Since the resistivity has the similarity as the Kondo effect, we also compute the DOS of the impurity electron

$$A_d(\omega) = -\frac{1}{\pi}\mathrm{Im}G_d(\omega + i\delta) = -\frac{1}{\pi}\mathrm{Im}\left[\frac{1}{\omega + i\delta - E_d + i\Delta - \Sigma(\omega + i\delta)}\right], \tag{20}$$

which is shown in Fig. 6. At the fixed impurity electron concentrations, peaks of the impurity electron DOS decrease versus temperature, and lines of $A_{\rm d}(\omega)$ become broad, as shown in Figs. 6(a)–6(d). The black solid lines of Figs. 6(a)–6(d) and 6(f) are the case that the system behaves as FL, the red dotted lines of Figs. 6(a)–6(d) and 6(f) are the case of $T = T^{\star}$, while blue dashed lines of Figs. 6(a)–6(d) and 6(f) are the case that the system behaves as the NFL. When $T = T^{\star}$, peaks of $A_{\rm d}(\omega)$ decrease versus $n_{\rm d}$, as shown in Fig. 6(e). In Fig. 6(f), both lines are similar to Figs. 6(a)–6(d), but $A_{\rm d}(\omega)$ has a smaller peak than Fig. 6(d) at $T^{\star}$ on account of the smaller conduction electron bandwidth.

Compared with the SYK model, our model has the hybridization between the conduction electrons and the impurity electron, while the standard SYK model does not have the hybridization, but the Lorentz lineshape of the impurity electron DOS is similar to the SYK model. Compared with the single-impurity Anderson model, our model has the random four-body SYK interaction between different pseudospin states of the impurity electron not the onsite Coulomb interaction between different impurity spins (spin up and spin down), which does not induce the sharp-peak like the Kondo resonance around the Fermi surface, while the single-impurity Anderson model has the Kondo resonance around the Fermi surface.[5,6,53,54]

4. Thermodynamics

The impurity electron contributes a free-energy as

$$\begin{aligned}\frac{F_{\rm d}}{N} &= -T\ln 2 - \frac{3}{4}T\sum_{n}\Sigma(\mathrm{i}\omega_n)G_{\rm d}(\mathrm{i}\omega_n)\\ &\quad + T\sum_{n}\left[\ln(-\beta G_{\rm d}(\mathrm{i}\omega_n)) - \ln(-\beta\,\mathrm{i}\omega_n)\right], \end{aligned} \tag{21}$$

while the conduction electron has an FG result $\frac{F_{\rm c}}{N} = -T\sum_k \ln(1+\mathrm{e}^{-\beta\varepsilon_k})$. In this way, the system's total free-energy F can be obtained by $\frac{F}{N} = \frac{F_{\rm c}}{N} + \frac{F_{\rm d}}{N} = -T\ln\mathcal{Z}$. The detailed derivation of the free-energy is given in the appendix.

Because conduction electrons only contribute trivial FG result, we focus on the thermodynamics of the impurity electron. Therefore, the impurity electron's entropy $S_{\rm d}$ and specific heat capacity $C_{\rm v}$ are given by

$$S_{\rm d} = -\frac{\partial F_{\rm d}}{\partial T}, \quad C_{\rm v} = T\frac{\partial S_{\rm d}}{\partial T} = -T\frac{\partial^2 F_{\rm d}}{\partial T^2}. \tag{22}$$

According to Eq. (18), the system behaves as an FL at low temperature, while at high temperature it is an NFL. Due to Refs. [24] and [48], there may exist a quantum phase transition in our model. We have got its entropy $S_{\rm d}$ and specific heat capacity $C_{\rm v}$ versus temperature T by Eq. (22), which is shown in Fig. 7. For intermediate-T, $S_{\rm d}$ increases with $n_{\rm d}$. All $S_{\rm d}$ gradually approach saturation at high-T limit with $\lim_{T\to\infty} S_{\rm d} = \ln 2$, as shown in Fig. 7(a).[39,61] $C_{\rm v}$ has a maximum at intermediate-T, which is similar to the SYK model.[39,62] $C_{\rm v}$ increases with $n_{\rm d}$ at low temperature, while it decreases for high temperature.

Since entropy and specific heat capacity are continuous and smooth, we expect a crossover, instead of phase transition, between FL and the NFL. Interestingly, similar transport properties also display in Kondo physics, and dilute magnetic alloy systems undergo a crossover from free local moment state to the non-magnetic FL state.[5,6]

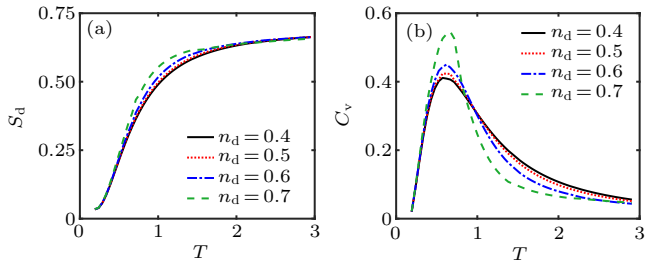


Fig. 7. The thermodynamics of our model as a function of temperature T, for different impurity electron concentrations $n_{\rm d}$. (a) The entropy $S_{\rm d}$ and (b) the specific heat capacity $C_{\rm v}$ of the impurity electron. The parameters are $V = 1$, $U = 3$, $D = 12$, $E_{\rm d} = -U/2$.

The two systems have similar transport and thermodynamics, and they undergo a crossover rather than phase transition.[5] Although both systems have the scattering between conduction electrons and the impurity electron, the DOS of the impurity electron is significantly different. Moreover, SYKAM has an NFL behavior $\rho_{\rm c}(T) \propto T$ at temperature $T > T^{\star}$, while the Kondo screening is the localized FL below Kondo temperature and the NFL behavior does not appear in the standard Anderson model. Since no symmetry-breaking is involved, a crossover is expected between the FL and the NFL, and thermodynamics can not be used to detect crossover due to the lack of singularity.

5. Renormalization group analysis

To proceed, we apply the RG theory to further confirm our results obtained above. We begin with the effective action Eq. (A9) by Fourier transformations, $d_i^{\dagger}(\tau) = \frac{1}{\sqrt{\beta}}\sum_n \mathrm{e}^{-\mathrm{i}\omega_n\tau} d_i^{\dagger}(\mathrm{i}\omega_n)$ and $d_i(\tau') = \frac{1}{\sqrt{\beta}}\sum_n \mathrm{e}^{\mathrm{i}\omega_n\tau'} d_i(\mathrm{i}\omega_n)$. We can get

$$\begin{aligned}\mathcal{S}_{\rm d} \simeq & -\frac{U^2}{4N^3(\sqrt{\beta})^8}\int \mathrm{d}\tau \int \mathrm{d}\tau' \sum_{ijml}\sum_{ns,s=1}^{8}\{d_i^{\dagger}(\mathrm{i}\omega_{n1})d_i(\mathrm{i}\omega_{n2})\\ &\times d_j^{\dagger}(\mathrm{i}\omega_{n3})d_j(\mathrm{i}\omega_{n4})d_m^{\dagger}(\mathrm{i}\omega_{n5})d_m(\mathrm{i}\omega_{n6})d_l^{\dagger}(\mathrm{i}\omega_{n7})d_l(\mathrm{i}\omega_{n8})\\ &\times \mathrm{e}^{[-\mathrm{i}(\omega_{n1}+\omega_{n3}-\omega_{n6}-\omega_{n8})\tau+\mathrm{i}(\omega_{n2}+\omega_{n4}-\omega_{n5}-\omega_{n7})\tau']}\}\\ = & -\frac{U^2 N}{4N^3(\sqrt{\beta})^8}\sum_{ns,s=1}^{8}\left[d_i^{\dagger}(\mathrm{i}\omega_{n1})d_i(\mathrm{i}\omega_{n2})d_j^{\dagger}(\mathrm{i}\omega_{n3})d_j(\mathrm{i}\omega_{n4})\right.\\ &\times d_m^{\dagger}(\mathrm{i}\omega_{n5})d_m(\mathrm{i}\omega_{n6})d_l^{\dagger}(\mathrm{i}\omega_{n7})d_l(\mathrm{i}\omega_{n8})\delta(\omega_{n1}-\omega_{n2}\\ &\left.+\omega_{n3}-\omega_{n4}+\omega_{n5}-\omega_{n6}+\omega_{n7}-\omega_{n8})\right]. \end{aligned} \tag{23}$$

In order to renormalize our model, we have a parameter λ ($\lambda > 1$) to cut off the fermionic Matsubara frequency ω_n and divide our model into the low energy part and the high energy

part as follows:

$$d_i^{\dagger}(\tau)=\frac{1}{\sqrt{\beta}}\sum_n \mathrm{e}^{-\mathrm{i}\omega_n\tau}\left(d_{iL}^{\dagger}(\mathrm{i}\omega_n)+d_{iH}^{\dagger}(\mathrm{i}\omega_n)\right), \quad (24)$$

$$d_i(\tau)=\frac{1}{\sqrt{\beta}}\sum_n \mathrm{e}^{\mathrm{i}\omega_n\tau}\left(d_{iL}(\mathrm{i}\omega_n)+d_{iH}(\mathrm{i}\omega_n)\right), \quad (25)$$

where $d_{iL}^{\dagger}(\mathrm{i}\omega_n)$ ($d_{iL}(\mathrm{i}\omega_n)$) denotes the low energy component of the system, $d_{iH}^{\dagger}(\mathrm{i}\omega_n)$ ($d_{iH}(\mathrm{i}\omega_n)$) is the system's high energy component. On the basis of the analytic continuation, it alludes to a cutoff energy $\omega_{\mathrm{F}}/\lambda$ ($\lambda>1$), the system is divided into the low energy component ($0<|\omega|<\omega_{\mathrm{F}}/\lambda$) and the high energy component ($\omega_{\mathrm{F}}/\lambda<|\omega|<\omega_{\mathrm{F}}$), and ω_{F} is the Fermi energy. We rescale the energy as

$$\omega'=\lambda\omega \quad (\lambda>1). \quad (26)$$

The effective action is given by

$$\mathcal{S}_{\mathrm{int}}\approx\mathcal{S}_L+\mathcal{S}_H+\mathcal{V}(L,H), \quad (27)$$

where $\mathcal{S}_L$ defines the low energy part of the effective action, $\mathcal{S}_H$ is the effective action for high energy component, and $\mathcal{V}(L,H)$ describes the coupling of the low and high energy components. Hence, the partition function of the system is $\mathcal{Z}=\mathcal{Z}_{\mathrm{c}}\mathcal{Z}_{\mathrm{f}}$, and $\mathcal{Z}_{\mathrm{f}}$ can be read as

$$\begin{aligned}\mathcal{Z}_{\mathrm{f}}\approx&\left[\int\mathcal{D}d\prod_{s=1}^{8}\int_0^{\frac{\omega_{\mathrm{F}}}{\lambda}}\mathrm{d}\omega_{\mathrm{s}}\,\mathrm{e}^{\mathcal{S}_L}\prod_{s=1}^{8}\int_{\frac{\omega_{\mathrm{F}}}{\lambda}}^{\omega_{\mathrm{F}}}\mathrm{d}\omega_{\mathrm{s}}\,\mathrm{e}^{\mathcal{S}_H}\right.\\&\left.\times\frac{\prod_{s=1}^{8}\int_{\frac{\omega_{\mathrm{F}}}{\lambda}}^{\omega_{\mathrm{F}}}\mathrm{d}\omega_{\mathrm{s}}\,\mathrm{e}^{\mathcal{S}_H}\,\mathrm{e}^{\mathcal{V}(L,H)}}{\prod_{s=1}^{8}\int_{\frac{\omega_{\mathrm{F}}}{\lambda}}^{\omega_{\mathrm{F}}}\mathrm{d}\omega_{\mathrm{s}}\,\mathrm{e}^{\mathcal{S}_H}}\right]\\=&\int\mathcal{D}d\prod_{s=1}^{8}\int_0^{\frac{\omega_{\mathrm{F}}}{\lambda}}\mathrm{d}\omega_{\mathrm{s}}\,\mathrm{e}^{\mathcal{S}_L}\prod_{s=1}^{8}\int_{\frac{\omega_{\mathrm{F}}}{\lambda}}^{\omega_{\mathrm{F}}}\mathrm{d}\omega_{\mathrm{s}}\,\mathrm{e}^{\mathcal{S}_H}\,\mathrm{e}^{\langle\mathcal{V}\rangle}, \quad (28)\end{aligned}$$

where

$$\mathrm{e}^{\langle\mathcal{V}\rangle}=\mathrm{e}^{\langle\mathcal{V}\rangle_0+\frac{1}{2}\langle\mathcal{V}^2\rangle_0+\mathcal{O}(\mathcal{V}^2)}, \quad (29)$$

$$\langle\mathcal{V}\rangle_0=\frac{\prod_{s=1}^{8}\int_{\frac{\omega_{\mathrm{F}}}{\lambda}}^{\omega_{\mathrm{F}}}\mathrm{d}\omega_{\mathrm{s}}\,\mathrm{e}^{\mathcal{S}_H}\mathcal{V}}{\prod_{s=1}^{8}\int_{\frac{\omega_{\mathrm{F}}}{\lambda}}^{\omega_{\mathrm{F}}}\mathrm{d}\omega_{\mathrm{s}}\,\mathrm{e}^{\mathcal{S}_H}}. \quad (30)$$

In the light of the first-order and second-order correction, the detailed calculations are shown in the appendix, and the RG transformation relation can be written as

$$\left(U'\right)^2=U^2\left[1+\frac{U^2\omega_{\mathrm{F}}^4}{2\Delta^4}\left(1-\frac{1}{\lambda}\right)^4\right]. \quad (31)$$

We set $\lambda=\mathrm{e}^l$, and its flow equation is

$$\frac{\mathrm{d}U^2}{\mathrm{d}l}=\frac{2U^4\omega_{\mathrm{F}}^4}{\Delta^4}. \quad (32)$$

In the fixed points, the scaling invariance has a consequence $\mathrm{d}U^2/\mathrm{d}l=0$; it demonstrates that SYKAM has two fixed points $U^2=0$ and $U^2=\infty$, as shown in Fig. 8. For $U^2=0$, it scales to a weak coupling repulsive fixed point, forming FG. $U^2=\infty$ is a strong coupling attractive fixed point of FL. Scaling proceeds from a repulsive fixed point via a crossover to an attractive fixed point, in which exists an NFL at finite U^2.

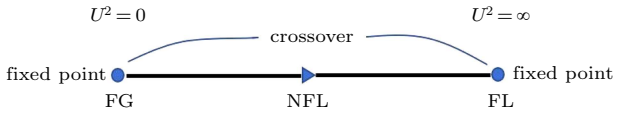


Fig. 8. Schematic illustration of RG flow in the SYKAM. For $U^2=0$, it scales to a weak coupling fixed point, forming the FG. $U^2=\infty$ is a strong coupling fixed point of FL. Here the weak and strong coupling does not mean the weak coupling limit and the strong coupling limit in this paper. Scaling proceeds from a repulsive fixed point via a crossover to an attractive fixed point, in which exists an NFL at finite U^2.

6. Summary and perspective

We have computed the transport and thermodynamics of SYKAM, which demonstrates that the NFL exists at temperature $T>T^{\star}$. The RG analysis shows a crossover between FG ($U^2=0$) and FL ($U^2=\infty$), which presents the NFL at finite U^2. The impurity electron's entropy S_{d} and the specific heat capacity C_{v} exhibit the similarity to the SYK model and the Kondo system.[5,39,62] The resistivity of SYKAM has a minimum at temperature $T^{\star}$, similar to Kondo temperature, but the impurity electron DOS of SYKAM does not have the sharp Kondo resonance peak around the Fermi surface.[5,6]

Our model is an extension of the single-impurity Anderson model and the SYK model. Comparing with the single-impurity Anderson model, the SYK random interaction can not provide the localized interaction to the onsite different impurity spin states, so our system does not form local moments. Compared to the SYK model, our system has the hybridization between the conduction electrons and impurity electron, which is present in the Kondo systems but does not exist in the SYK model. The resistivity minimum emerges in SYKAM when it behaves like an NFL, where the impurity electron has the SYK interaction without Coulomb interaction. Anderson model and our model both have the scattering between the conduction electrons and the impurity electron because of the hybridization, and except that the DOS of the impurity electron does not display the sharp-peak as the Kondo resonance and not have the localized magnetic moments in SYKAM.

Finally, it may be helpful to lead to a new route to realize the Kondo systems (heavy-fermion compounds, various quantum dot devices, and novel material Kondo systems) and the SYK physics. With the development of ultracold atom technique for realizing the Kondo lattice model,[63–65] our results may be protocolled in near-future experiments.

Appendix A: Transport properties

When $|\omega|\ll E^{\star}$, it shows FL-like behavior, Green's function of the impurity electron and the conduction electron, i.e., ($T=0$)

$$G_{\mathrm{d}}(\omega)=\begin{cases}\dfrac{1}{\omega+\mathrm{i}\Delta+\left(\dfrac{U}{\pi\Delta}\right)^2\omega+\mathrm{i}\dfrac{U^2\pi}{2(\pi\Delta)^3}\omega^2}, & |\omega|\ll E^{\star},\\ \dfrac{\pi^{1/4}}{\sqrt{2U}}\dfrac{1}{\sqrt{|\omega|}}, & |\omega|\gg E^{\star}.\end{cases} \quad (A1)$$

$$G_{\rm c}(k,\omega)=\begin{cases}\dfrac{1}{\omega-\varepsilon_k}+\dfrac{V^2}{(\omega-\varepsilon_k)^2}\dfrac{1}{\left[\omega+{\rm i}\Delta+\left(\dfrac{U}{\pi\Delta}\right)^2\omega+{\rm i}\dfrac{U^2\pi}{2(\pi\Delta)^3}\omega^2\right]}, & |\omega|\ll E^\star,\\ \dfrac{1}{\omega-\varepsilon_k}+\dfrac{V^2}{(\omega-\varepsilon_k)^2}\dfrac{\pi^{1/4}}{\sqrt{2U}}\dfrac{1}{\sqrt{|\omega|}}, & |\omega|\gg E^\star.\end{cases}\tag{A2}$$

The spectral function of conduction electrons is

$$\begin{aligned}&A_{\rm c}(k,\varepsilon_1)\\&=-\frac{1}{\pi}{\rm Im}G_{\rm c}({\rm k},\varepsilon_1+{\rm i}\delta)\\&=-\frac{1}{\pi}{\rm Im}\left[\frac{1}{\varepsilon_1+{\rm i}\delta-\varepsilon_{\rm k}}+\frac{{\rm V}^2}{(\varepsilon_1+{\rm i}\delta-\varepsilon_{\rm k})^2}{\rm G_d}(\varepsilon_1+{\rm i}\delta)\right]\\&=\frac{V^2}{(\varepsilon_1-\varepsilon_k)^2}\left[-\frac{1}{\pi}{\rm Im}G_{\rm d}(\varepsilon_1+{\rm i}\delta)\right]\\&\quad+\frac{(\varepsilon_1-\varepsilon_k)[\varepsilon_1-E_{\rm d}-\Sigma(\varepsilon_1)]\delta(\varepsilon_1-E_{\rm d}-\Sigma(\varepsilon_1))}{(\varepsilon_1-\varepsilon_k)[\varepsilon_1-E_{\rm d}-\Sigma(\varepsilon_1)]-V^2}\\&\simeq\frac{V^2}{(\varepsilon_1-\varepsilon_k)^2}A_{\rm d}(\varepsilon_1),\end{aligned}\tag{A3}$$

where we omit the term $\frac{(\varepsilon_1-\varepsilon_k)[\varepsilon_1-E_{\rm d}-\Sigma(\varepsilon_1)]\delta(\varepsilon_1-E_{\rm d}-\Sigma(\varepsilon_1))}{(\varepsilon_1-\varepsilon_k)[\varepsilon_1-E_{\rm d}-\Sigma(\varepsilon_1)]-V^2}$ because of small contribution of $A_{\rm c}(k,\varepsilon_1)$.[58]

We assume that $(\partial\varepsilon_k/\partial k_x)^2=v_{\rm F}^2$ at the low energy scale, where $v_{\rm F}$ is the Fermi velocity. Thus, we can just compute the integral $\sum_{kj}[A_{\rm c}(k,\varepsilon_1)]^2$. We have

$$\begin{aligned}&\sum_{kj}[A_{\rm c}(k,\varepsilon_1)]^2\\&=\sum_{kj}\int_{-D}^{D}{\rm d}E\delta(E-\varepsilon_k)\,[A_{\rm c}(k,\varepsilon_1)]^2\\&=\int_{-D}^{D}{\rm d}EN(E)\frac{V^4}{(\varepsilon_1-E)^4}A_{\rm d}^2(\varepsilon_1)\\&\simeq\int_{-D}^{D}{\rm d}EN(0)\frac{V^4}{(\varepsilon_1-E)^4}A_{\rm d}^2(\varepsilon_1)\\&=\frac{V^4}{3}A_{\rm d}^2(\varepsilon_1)N(0)\left[\frac{1}{(\varepsilon_1-D)^3}-\frac{1}{(\varepsilon_1+D)^3}\right].\end{aligned}\tag{A4}$$

Thus, the conduction electron concentration is given by

$$n_{\rm c}=\sum_k\int{\rm d}\omega A_{\rm c}(k,\omega)f(\omega),\tag{A5}$$

where $f(x)=1/[{\rm e}^{(x-\mu)/T}+1]$ is the Fermi–Dirac distribution function, μ is the total system's chemical potential since our system has two types of electrons (conduction and the impurity electrons), and we approximate it by conduction electron chemical potential $\mu_{\rm c}$ in our work.

According to Eq. (16), we have presented the conduction electron resistivity $\rho_{\rm c}$ versus temperature T with fixed $n_{\rm d}$ (tuning the chemical potential), as shown in Figs. 4 and 5. However, when we fix $n_{\rm c}$ by tuning the chemical potential, the conduction electron resistivity $\rho_{\rm c}$ is changed versus temperature T. We have plot conduction electron resistivity $\rho_{\rm c}$ as a function of temperature T at the conduction electron concentration $n_{\rm c}=0.4$, as shown in Fig. A1. It shows that the conduction electron resistivity $\rho_{\rm c}$ emerges a minimum versus temperature T when fixed the conduction electron occupation $n_{\rm c}$, which behaves like that in the Kondo effect.[5,6,60]

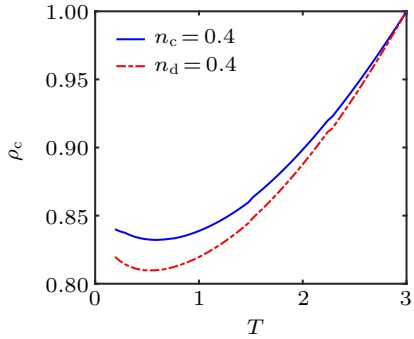


Fig. A1. The conduction electron resistivity $\rho_{\rm c}$ as a function of temperature T at the conduction electron concentration $n_{\rm c}=0.4$, the red dashed line is the impurity electron concentration $n_{\rm d}=0.4$, the parameters are $V=1$, $U=3$, $D=12$, $E_{\rm d}=-U/2$.

Appendix B: Thermodynamics

Thermodynamics of our model is determined by the partition function $\mathcal{Z}$, whose functional integral formalism is

$$\mathcal{Z}=\int\mathcal{D}c^\dagger\mathcal{D}c\mathcal{D}d^\dagger\mathcal{D}d\,{\rm e}^{-\mathcal{S}_0-\mathcal{S}_{\rm int}}.\tag{A6}$$

Here the non-interacting action is

$$\begin{aligned}\mathcal{S}_0=\int{\rm d}\tau\Bigg[&\sum_{kj}c_{kj}^\dagger(\partial_\tau+\varepsilon_k)c_{kj}+V\sum_{kj}c_{kj}^\dagger d_j\\&+V\sum_{kj}d_j^\dagger c_{kj}+\sum_j d_j^\dagger(\partial_\tau+E_{\rm d})d_j\Bigg],\end{aligned}\tag{A7}$$

with imaginary time $\tau\in[0,\beta]$ ($\beta=1/T$) and c_{kj}, d_j are the anticommuting Grassman fields. The SYK interaction reads

$$\mathcal{S}_{\rm int}=-\frac{1}{(2N)^{3/2}}\int{\rm d}\tau\sum_{ijml}U_{ijml}d_i^\dagger d_j^\dagger d_m d_l.\tag{A8}$$

After performing the standard Gaussian random average over each independent U_{ijml} and focusing on one replica realization,[46] we obtain

$$\begin{aligned}\mathcal{S}_{\rm int}=-\frac{U^2}{4N^3}\int{\rm d}\tau\int{\rm d}\tau'\sum_{ijml}\big[&d_i^\dagger(\tau)d_i(\tau')\\&\times d_j^\dagger(\tau)d_j(\tau')d_m^\dagger(\tau')d_m(\tau)d_l^\dagger(\tau')d_l(\tau)\big].\end{aligned}\tag{A9}$$

Now we introduce $G_{\rm d}(\tau',\tau)=\frac{1}{N}\sum_j d_j^\dagger(\tau)d_j(\tau')$ and a Lagrange multiplier $\Sigma(\tau,\tau')$ into the action $\mathcal{S}_{\rm int}$ with adding the following constraint term into the partition function

$$\begin{aligned}1&=\int\mathcal{D}G\delta\left(G_{\rm d}(\tau',\tau)-\frac{1}{N}\sum_j d_j^\dagger(\tau)d_j(\tau')\right)\\&=\int\mathcal{D}\Sigma\int\mathcal{D}G\mathrm{e}^{\int\mathrm{d}\tau\int\mathrm{d}\tau'\Sigma(\tau,\tau')\left[NG_{\rm d}(\tau',\tau)-\sum_j d_j^\dagger(\tau)d_j(\tau')\right]}.\end{aligned}\tag{A10}$$

Therefore, we can rewrite $\mathcal{S}_{\rm int}$ as

$$\begin{aligned}\mathcal{S}_{\rm d}=&\int\mathrm{d}\tau\int\mathrm{d}\tau'\Bigg\{\sum_j d_j^\dagger(\tau)\Bigg[\Sigma(\tau,\tau')+\Bigg(\partial_{\tau'}+E_{\rm d}\\&-\sum_k V^2(\partial_\tau+\varepsilon_k)^{-1}\Bigg)\delta(\tau-\tau')\Bigg]d_j(\tau')\Bigg\}\\&-N\int\mathrm{d}\tau\int\mathrm{d}\tau'\Sigma(\tau,\tau')G_{\rm d}(\tau,\tau')\\&-\frac{NU^2}{4}\int\mathrm{d}\tau\int\mathrm{d}\tau'|G_{\rm d}(\tau,\tau')|^4,\end{aligned}\tag{A11}$$

where $\mathcal{S}_{\rm d}$ is the effective action for G and Σ. In the large-N limit, the partition function is dominated by the extremal $\mathcal{S}_{\rm d}$, which leads to Eqs. (3) and (2) via the saddle point equations

$$\frac{\delta\mathcal{S}_{\rm d}}{\delta G}=0,\quad\frac{\delta\mathcal{S}_{\rm d}}{\delta\Sigma}=0.\tag{A12}$$

According to Eq. (2), we can get the effective action

$$\begin{aligned}\mathcal{S}_{\rm d}=&-N\ln\mathrm{Det}\left[\left(\partial_{\tau'}+E_{\rm d}-\sum_k\frac{V^2}{\partial_\tau+\varepsilon_k}\right)\delta(\tau-\tau')+\Sigma(\tau,\tau')\right]\\&-N\int\mathrm{d}\tau\int\mathrm{d}\tau'\Sigma(\tau,\tau')G_{\rm d}(\tau',\tau)\\&-\frac{NU^2}{4}\int\mathrm{d}\tau\int\mathrm{d}\tau'|G_{\rm d}(\tau,\tau')|^4\\=&N\mathrm{Tr}[\ln(G_{\rm d}(\tau,\tau'))]-N\mathrm{Tr}[\ln(G_{\rm d}^0(\tau,\tau'))]\\&+N\mathrm{Tr}\left[\ln(G_{\rm d}^0(\tau,\tau'))\right]\\&-\frac{3N}{4}\int\mathrm{d}\tau\int\mathrm{d}\tau'\Sigma(\tau,\tau')G_{\rm d}(\tau',\tau)\\=&-N\ln 2-\frac{3N}{4}\sum_n\Sigma(\mathrm{i}\omega_n)G_{\rm d}(\mathrm{i}\omega_n)\\&+N\sum_n\Big[\ln(-\beta G_{\rm d}(\mathrm{i}\omega_n))-\ln(-\beta\mathrm{i}\omega_n)\Big].\end{aligned}\tag{A13}$$

Therefore, we can get the free-energy of impurity electron

$$\begin{aligned}\frac{F_{\rm d}}{N}=&-T\ln\mathcal{Z}\\=&-T\ln 2-\frac{3}{4}T\sum_n\Sigma(\mathrm{i}\omega_n)G_{\rm d}(\mathrm{i}\omega_n)\\&+T\sum_n\Big[\ln(-\beta G_{\rm d}(\mathrm{i}\omega_n))-\ln(-\beta\mathrm{i}\omega_n)\Big].\end{aligned}\tag{A14}$$

Appendix C: Renormalization group analysis

According to Eq. (29), we can compute the leading order Feynman diagrams as shown in Fig. C1.

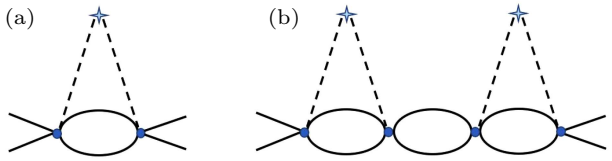


Fig. C1. The leading Feynman diagrams of our model to compute the RG transformation relation Eq. (31). (a) is the first order and (b) is the second order.

The first order $\langle\mathcal{V}\rangle_0$ have two terms: $\langle d_{iL}^\dagger(\mathrm{i}\omega_{n1})d_{iL}(\mathrm{i}\omega_{n2})d_{jL}^\dagger(\mathrm{i}\omega_{n3})d_{jL}(\mathrm{i}\omega_{n4})d_{mL}^\dagger(\mathrm{i}\omega_{n5})d_{mL}(\mathrm{i}\omega_{n6})d_{lL}^\dagger(\mathrm{i}\omega_{n7})d_{lL}(\mathrm{i}\omega_{n8})\rangle_0$, $\langle d_{iH}^\dagger(\mathrm{i}\omega_{n1})d_{iH}(\mathrm{i}\omega_{n2})d_{jH}^\dagger(\mathrm{i}\omega_{n3})d_{jH}(\mathrm{i}\omega_{n4})d_{mH}^\dagger(\mathrm{i}\omega_{n5})d_{mH}(\mathrm{i}\omega_{n6})d_{lH}^\dagger(\mathrm{i}\omega_{n7})d_{lH}(\mathrm{i}\omega_{n8})\rangle_0$. The low energy part is a constat.

The second order $\langle\mathcal{V}^2\rangle_0$ have four terms: $\langle d_{iL}^\dagger(\mathrm{i}\omega_{n1})d_{iL}(\mathrm{i}\omega_{n2})d_{jL}^\dagger(\mathrm{i}\omega_{n3})d_{jL}(\mathrm{i}\omega_{n4})d_{mL}^\dagger(\mathrm{i}\omega_{n5})d_{mL}(\mathrm{i}\omega_{n6})d_{lL}^\dagger(\mathrm{i}\omega_{n7})$ $d_{lL}(\mathrm{i}\omega_{n8})d_{iL}^\dagger(\mathrm{i}\omega_{n9})d_{iL}(\mathrm{i}\omega_{n10})d_{jL}^\dagger(\mathrm{i}\omega_{n11})d_{jL}(\mathrm{i}\omega_{n12})d_{mL}^\dagger(\mathrm{i}\omega_{n13})d_{mL}(\mathrm{i}\omega_{n14})d_{lL}^\dagger(\mathrm{i}\omega_{n15})d_{lL}(\mathrm{i}\omega_{n16})\rangle_0$, $\langle d_{iL}^\dagger(\mathrm{i}\omega_{n1})d_{iL}(\mathrm{i}\omega_{n2})$ $d_{jL}^\dagger(\mathrm{i}\omega_{n3})d_{jL}(\mathrm{i}\omega_{n4})d_{mL}^\dagger(\mathrm{i}\omega_{n5})d_{mL}(\mathrm{i}\omega_{n6})d_{lL}^\dagger(\mathrm{i}\omega_{n7})d_{lL}(\mathrm{i}\omega_{n8})d_{iH}^\dagger(\mathrm{i}\omega_{n9})d_{iH}(\mathrm{i}\omega_{n10})d_{jH}^\dagger(\mathrm{i}\omega_{n11})d_{jH}(\mathrm{i}\omega_{n12})d_{mH}^\dagger(\mathrm{i}\omega_{n13})$ $d_{mH}(\mathrm{i}\omega_{n14})d_{lH}^\dagger(\mathrm{i}\omega_{n15})d_{lH}(\mathrm{i}\omega_{n16})\rangle_0$, $\langle d_{iH}^\dagger(\mathrm{i}\omega_{n1})d_{iH}(\mathrm{i}\omega_{n2})d_{jH}^\dagger(\mathrm{i}\omega_{n3})d_{jH}(\mathrm{i}\omega_{n4})d_{mH}^\dagger(\mathrm{i}\omega_{n5})d_{mH}(\mathrm{i}\omega_{n6})d_{lH}^\dagger(\mathrm{i}\omega_{n7})d_{lH}(\mathrm{i}\omega_{n8})$ $d_{iL}^\dagger(\mathrm{i}\omega_{n9})d_{iL}(\mathrm{i}\omega_{n10})d_{jL}^\dagger(\mathrm{i}\omega_{n11})d_{jL}(\mathrm{i}\omega_{n12})d_{mL}^\dagger(\mathrm{i}\omega_{n13})d_{mL}(\mathrm{i}\omega_{n14})d_{lL}^\dagger(\mathrm{i}\omega_{n15})d_{lL}(\mathrm{i}\omega_{n16})\rangle_0$, $\langle d_{iH}^\dagger(\mathrm{i}\omega_{n1})d_{iH}(\mathrm{i}\omega_{n2})d_{jH}^\dagger(\mathrm{i}\omega_{n3})$ $d_{jH}(\mathrm{i}\omega_{n4}d_{mH}^\dagger(\mathrm{i}\omega_{n5})d_{mH}(\mathrm{i}\omega_{n6})d_{lH}^\dagger(\mathrm{i}\omega_{n7})d_{lH}(\mathrm{i}\omega_{n8})d_{iH}^\dagger(\mathrm{i}\omega_{n9})d_{iH}(\mathrm{i}\omega_{n10})d_{jH}^\dagger(\mathrm{i}\omega_{n11})d_{jH}(\mathrm{i}\omega_{n12})d_{mH}^\dagger(\mathrm{i}\omega_{n13})d_{mH}(\mathrm{i}\omega_{n14})$ $d_{lH}^\dagger(\mathrm{i}\omega_{n15})d_{lH}(\mathrm{i}\omega_{n16})\rangle_0$. Here the low energy part is a constant, and the high energy part is omitted. We just compute the low energy and high energy hybridized terms. Since the second term is equal to the third term, we have

$$\begin{aligned}&\langle d_{iH}^\dagger(\mathrm{i}\omega_{n1})d_{iH}(\mathrm{i}\omega_{n2})d_{jH}^\dagger(\mathrm{i}\omega_{n3})d_{jH}(\mathrm{i}\omega_{n4})d_{mH}^\dagger(\mathrm{i}\omega_{n5})d_{mH}(\mathrm{i}\omega_{n6})d_{lH}^\dagger(\mathrm{i}\omega_{n7})d_{lH}(\mathrm{i}\omega_{n8})d_{iL}^\dagger(\mathrm{i}\omega_{n9})d_{iL}(\mathrm{i}\omega_{n10})\\&d_{jL}^\dagger(\mathrm{i}\omega_{n11})d_{jL}(\mathrm{i}\omega_{n12})d_{mL}^\dagger(\mathrm{i}\omega_{n13})d_{mL}(\mathrm{i}\omega_{n14})d_{lL}^\dagger(\mathrm{i}\omega_{n15})d_{lL}(\mathrm{i}\omega_{n16})\rangle_0\\=&\frac{1}{\int\mathcal{D}d\sum_{ns=1}^8\mathrm{e}^{\mathcal{S}_H}}\int\mathcal{D}d\sum_{ns=1}^{16}\left[\mathrm{e}^{\mathcal{S}_H}d_{iH}^\dagger(\mathrm{i}\omega_{n1})d_{iH}(\mathrm{i}\omega_{n2})d_{jH}^\dagger(\mathrm{i}\omega_{n3})d_{jH}(\mathrm{i}\omega_{n4})d_{mH}^\dagger(\mathrm{i}\omega_{n5})d_{mH}(\mathrm{i}\omega_{n6})d_{lH}^\dagger(\mathrm{i}\omega_{n7})\right.\\&\left.d_{lH}(\mathrm{i}\omega_{n8})d_{iL}^\dagger(\mathrm{i}\omega_{n9})d_{iL}(\mathrm{i}\omega_{n10})d_{jL}^\dagger(\mathrm{i}\omega_{n11})d_{jL}(\mathrm{i}\omega_{n12})d_{mL}^\dagger(\mathrm{i}\omega_{n13})d_{mL}(\mathrm{i}\omega_{n14})d_{lL}^\dagger(\mathrm{i}\omega_{n15})d_{lL}(\mathrm{i}\omega_{n16})\right]\\=&\frac{1}{\int\mathcal{D}d\sum_{ns=1}^8\mathrm{e}^{\mathcal{S}_H}}\int\mathcal{D}d\sum_{ns=1}^{16}\left[\left(\mathrm{e}^{\mathcal{S}_H}\frac{\delta(\omega_{n1}-\omega_{n2})}{\mathrm{i}\omega_{n1}-E_{\rm d}+\mathrm{i}\Delta}\right)\left(\frac{\delta(\omega_{n3}-\omega_{n4})}{\mathrm{i}\omega_{n3}-E_{\rm d}+\mathrm{i}\Delta}\right)\left(\frac{\delta(\omega_{n5}-\omega_{n6})}{\mathrm{i}\omega_{n3}-E_{\rm d}+\mathrm{i}\Delta}\right)\left(\frac{\delta(\omega_{n7}-\omega_{n8})}{\mathrm{i}\omega_{n7}-E_{\rm d}+\mathrm{i}\Delta}\right)\right.\end{aligned}$$

$$d_{iL}(\mathrm{i}\omega_{n10})d^{\dagger}_{iL}(\mathrm{i}\omega_{n9})d_{jL}(\mathrm{i}\omega_{n12})d^{\dagger}_{jL}(\mathrm{i}\omega_{n11})d_{mL}(\mathrm{i}\omega_{n14})d^{\dagger}_{mL}(\mathrm{i}\omega_{n13})d_{lL}(\mathrm{i}\omega_{n16})d^{\dagger}_{lL}(\mathrm{i}\omega_{n15})\Big]$$

$$\simeq \int \mathcal{D}d \int_{\omega_{\mathrm{F}}/\lambda}^{\omega_{\mathrm{F}}} \mathrm{d}\omega_1 \int_{\omega_{\mathrm{F}}/\lambda}^{\omega_{\mathrm{F}}} \mathrm{d}\omega_3 \int_{\omega_{\mathrm{F}}/\lambda}^{\omega_{\mathrm{F}}} \mathrm{d}\omega_5 \int_{\omega_{\mathrm{F}}/\lambda}^{\omega_{\mathrm{F}}} \mathrm{d}\omega_7 \Bigg[\left(\frac{1}{\omega_1 - E_{\mathrm{d}} + \mathrm{i}\Delta}\right) \left(\frac{1}{\omega_3 - E_{\mathrm{d}} + \mathrm{i}\Delta}\right) \left(\frac{1}{\omega_5 - E_{\mathrm{d}} + \mathrm{i}\Delta}\right) \left(\frac{1}{\omega_7 - E_{\mathrm{d}} + \mathrm{i}\Delta}\right) d_{iL}(\mathrm{i}\omega_{n10})$$

$$d^{\dagger}_{iL}(\mathrm{i}\omega_{n9})d_{jL}(\mathrm{i}\omega_{n12})d^{\dagger}_{jL}(\mathrm{i}\omega_{n11})d_{mL}(\mathrm{i}\omega_{n14})d^{\dagger}_{mL}(\mathrm{i}\omega_{n13})d_{lL}(\mathrm{i}\omega_{n16})d^{\dagger}_{lL}(\mathrm{i}\omega_{n15})\Bigg]$$

$$\approx \int \mathcal{D}d \left[\frac{(\omega_{\mathrm{F}} - \frac{\omega_{\mathrm{F}}}{\lambda})^4}{(\mathrm{i}\Delta - E_{\mathrm{d}})^4} d_{iL}(\mathrm{i}\omega_{n10})d^{\dagger}_{iL}(\mathrm{i}\omega_{n9})d_{jL}(\mathrm{i}\omega_{n12})d^{\dagger}_{jL}(\mathrm{i}\omega_{n11})d_{mL}(\mathrm{i}\omega_{n14})d^{\dagger}_{mL}(\mathrm{i}\omega_{n13})d_{lL}(\mathrm{i}\omega_{n16})d^{\dagger}_{lL}(\mathrm{i}\omega_{n15}) \right]. \tag{A15}$$

Here, $\dfrac{1}{\omega_{\mathrm{s}} - E_{\mathrm{d}} + \mathrm{i}\Delta} \approx \dfrac{1}{-E_{\mathrm{d}} + \mathrm{i}\Delta}$, and $s = 1, 3, 5, 7$.

References

[1] Wilson K G 1975 *Rev. Mod. Phys.* **47** 773
[2] Krishna-murthy H R, Wilkins J W and Wilson K G 1980 *Phys. Rev. B* **21** 1003
[3] Krishna-murthy H R, Wilkins J W and Wilson K G 1980 *Phys. Rev. B* **21** 1044
[4] Krishna-murthy H R, Wilson K G and Wilkins J W 1975 *Phys. Rev. Lett.* **35** 1101
[5] Hewson A C 1997 *The Kondo Problem to Heavy Fermions* (Cambridge University Press)
[6] Coleman P 2015 *Introduction to Many-Body Physics* (Cambridge University Press)
[7] Coleman P 2006 arXiv:cond-mat/0612006v3
[8] Anderson P W 1961 *Phys. Rev.* **124** 41
[9] Schrieffer J R and Wolff P A 1966 *Phys. Rev.* **149** 491
[10] Kondo J 1964 *Prog. Theor. Phys.* **32** 37
[11] Chubukov A V 1964 *Physics* **3** 70
[12] Schroder A, Aeppli G, Coldea R, Adams M, Stockert O, Lohneysen H, Bucher E, Ramazashvili R and Coleman P 2000 *Nature* **407** 351
[13] Custers J, Gegenwart P, Wilhelm H, Neumaier K, Tokiwa Y, Trovarelli O, Geibel C, Steglich F, Pepin C and Coleman P 2003 *Nature* **424** 524
[14] Matsumoto Y, Nakatsuji S, Kuga K, Karaki Y, Horie N, Shimura Y, Sakakibara T, Nevidomskyy A H and Coleman P 2011 *Science* **331** 316
[15] Cubrovic M, Zaanen J and Schalm K 2009 *Science* **325** 439
[16] Si Q, Rabello S, Ingersent K and Smith J L 2001 *Nature* **413** 804
[17] Lee P A, Nagaosa N and Wen X G 2006 *Rev. Mod. Phys.* **78** 17
[18] Pepin C 2005 *Phys. Rev. Lett.* **94** 066402
[19] Senthil T, Sachdev S and Vojta M 2003 *Phys. Rev. Lett.* **90** 216403
[20] Senthil T, Sachdev S and Vojta M 2004 *Phys. Rev. B* **69** 035111
[21] Senthil Y F and Pines D 2014 *Proc. Natl. Acad. Sci.* **111** 8398
[22] Chowdhury D, Werman Y, Berg E and Senthil T 2018 *Phys. Rev. X* **8** 031024
[23] Haldar A, Banerjee S and Shenoy V B 2018 *Phys. Rev. B* **97** 241106
[24] Bi Z, Jian C M, You Y Z, Pawlak K A and Xu C 2017 *Phys. Rev. B* **95** 205105
[25] Ben-Zion D and McGreevy J 2018 *Phys. Rev. B* **97** 155117
[26] Sachdev S and Ye J 1993 *Phys. Rev. Lett.* **70** 3339
[27] Parcollet O and Georges A 1999 *Phys. Rev. B* **59** 5341
[28] Georges A, Parcollet O and Sachdev S 2000 *Phys. Rev. Lett.* **85** 840
[29] Georges A, Parcollet O and Sachdev S 2001 *Phys. Rev. B* **63** 134406
[30] Camjayi A and Rozenberg M J 2003 *Phys. Rev. Lett.* **90** 217202
[31] Kitaev A 2015 http://online.kitp.ucsb.edu/online/entangled15/kitaev/
[32] Kitaev A 2015 http://online.kitp.ucsb.edu/online/entangled15/kitaev2/
[33] Berkooz M, Narayan P, Rozali M and Simon J 2017 *J. High Energy Phys.* **1** 138
[34] Gu Y, Qi X L and Standford D 2017 *J. High Energy Phys.* **5** 125
[35] Sachdev S 2010 *Phys. Rev. Lett.* **105** 151602
[36] Polchinski J and Rosenhaus V 2016 *J. High Energy Phys.* **4** 1029
[37] Sachdev S 2015 *Phys. Rev. X* **5** 041025
[38] Maldacena J and Standford D 2016 *Phys. Rev. D* **94** 106002
[39] Pikulin D and Franz M 2017 *Phys. Rev. X* **7** 031006
[40] Fu D, Gaiotto D, Maldacena J and Sachdev S 2017 *Phys. Rev. D* **95** 026009
[41] Kukuljan I, Grozdanov S and Prosen T 2017 *Phys. Rev. B* **96** 060301
[42] Zhang P 2017 *Phys. Rev. B* **96** 205138
[43] Hosur P, Qi X L, Roberts D A and Yoshida B 2016 *J. High Energy Phys.* **2** 1029
[44] Jian S K and Yao H 2017 *Phys. Rev. Lett.* **119** 206602
[45] You Y Z, Ludwig A W W and Xu C 2017 *Phys. Rev. B* **95** 115150
[46] Song X Y, Jian C W and Balents L 2017 *Phys. Rev. Lett.* **119** 216601
[47] Patel A A, McGreevy J, Arovas D P and Sachdev S 2018 *Phys. Rev. X* **8** 021049
[48] Banerjee S and Altman E 2017 *Phys. Rev. B* **95** 134302
[49] Chen X, Fan R, Chen Y, Zhai H and Zhang P 2017 *Phys. Rev. Lett.* **119** 207603
[50] Jian S K, Xian Z Y and Yao H 2018 *Phys. Rev. B* **97** 205141
[51] Haldar A and Shenoy V B 2018 *Phys. Rev. B* **98** 165135
[52] Zhong Y 2018 *Journal of Physics Communications* **2** 095014
[53] Bickers N E, Cox L D and Wilkins J W 1987 *Phys. Rev. B* **36** 2036
[54] Bickers N E, Cox L D and Wilkins J W 1985 *Phys. Rev. Lett.* **54** 230
[55] Li Z Z 2002 *Solid State Theory* (Higher Education Press) (in Chinese)
[56] Abrikosov A A, Gorkov L P and Dzyaloshinski I E 1964 *Methods of Quantum Field Theory in Statistical Physics* (Prentice-Hall)
[57] Czycholl G and Leder H J 1981 *Zeitschrift fur Physik B* **44** 59
[58] Newns D M and Read N 1987 *Adv. Phys.* **36** 799
[59] Ashcroft N W and Mermin N D 1976 *Solid State Physics* (Horcort University Publishers)
[60] Sarachik M P, Corenzwit E and Longinotti L D 1964 *Phys. Rev.* **135** A1041
[61] Fu W and Sachdev S 2016 *Phys. Rev. B* **94** 035135
[62] Danshita I, Hanada M and Tezuka M 2017 *Prog. Theor. Exp. Phys.* **2017** 083
[63] Chin C, Grimm R, Julienne P and Tiesinga E 2010 *Rev. Mod. Phys.* **82** 1225
[64] Foss-Feig M and Rey A M 2011 *Phys. Rev. A* **84** 053619
[65] Isaev L and Rey A M 2015 *Phys. Rev. Lett.* **115** 165302